



## Effective Automated Controlled System for Sorting of Classified Ceramic Tiles Surface Defects

Monday F. Ohemu<sup>1</sup>, Zuleihat O. Zubair<sup>2</sup>, Charles B. Dyaji<sup>1</sup>, Rexcharles E. Donatus<sup>3</sup>

<sup>1</sup> Department of Electrical and Electronics Engineering,  
Airforce Institute of Technology, Kaduna, Nigeria

<sup>2</sup> Department of Physics,  
Nigerian Defense Academy, Kaduna, Nigeria

<sup>3</sup> Department Aerospace Engineering,  
Airforce Institute of Technology, Kaduna Nigeria

### ABSTRACT

Defects in ceramic tiles appear in various degrees and quality assurance CT companies try to use an automated system to detect, classify and sort them. To completely eliminate human intervention in the sorting stage along with production, detection, and classification stages, an automated control model is proposed so that the classified defective tiles are sorted automatically and returned for reprocessing. The sorting unit has four gates controlled by different motors that respond to a particular type of defect as indicated by the multi-class support vector machine classifier (SVM) whose output determines each motor's response. The result shows that each defect passes through the corresponding gate at a precise distance a PID controller is used than when only a DC motor is used. The result shows a better response time and overshoots with the PID controller than when the DC motor alone was used.

### ARTICLE INFO

Article History

Received: March, 2022

Received in revised form: March, 2022

Accepted: May, 2022

Published online: June, 2022

### KEYWORDS

Ceramic Tiles, DC, PID Controller, Support Vector Machine

### INTRODUCTION

The production chain of Ceramic tile undergoes numerous processes and any error in each of the process may result in defective product that should not come out of the factory as a means of quality control. Automated systems are been developed to detect, classified and sort the defects in the firing unit of the production process for prompt decision on preventing defective tiles to be mixed with the good ones. The defects are sometimes inconsistent and sometimes may not be easy to see, these makes ceramic tiles (CT) industries to find various innovative ways to overcome this challenge. Most factories depend on manual ways to detect, classify and sort out defective CT that is highly prone to error. (Hanzaei *et al.*, 2017).

When human being are used to manually detect these defective tiles, errors are inevitable and there are also exposed to factory hazards, when they begin to judge wrongly and this will result in CT omission (Meena, & Mittal, 2013). When there is error in defect detection, there will be error in classification of same and this will also lead to error in the defect sorting. The entire process need to be automated for effectiveness of

the production process to improve quality control (QC).

Detection and classification of CT stages of defect system have witnessed different approaches. Three main approaches have been used to detect defect in CT which are; statistical approaches, structural approach, and filter based method (Junmo *et al.*, 2005). In the statistical approach such as the histogram curve reported in (Latif-Amet *et al.*, 2000), for defect detection luminance histogram is used mostly and this method is often characterized with low complexity and simplicity. Apart from luminance histogram, another statistical approach is the Local Binary Pattern (LBP) which has higher computational time and better accuracy (Iivarinen, 2000). Structural method consist of conventional morphological operations (Mallik-Goswami & Datta 2000), while filter base method compose of partial domain filter and frequency domain filter like Gaussian and Canny filters (Vasilic and Hocenski, 2006) One of the best approach in detection of CT surface defect is the combination of statically approach and the morphological operation employed in (Hanzaei *et al.*, 2017). They used statistical method known as Rotation Invariant Measure of Local Variance (RIMLV) operator and for filling and smoothing the

detected region morphological operator was used. They used geometric descriptor to extract features used to train the classifier.

Monday *et al.*, 2021, adopted the method of (Hanzaei *et al.*, 2017) to detect the CT defect but used Fourier descriptors to extract the defect features that was used to train the Support vector machine (SVM) used to classify the defects. He recorded better accuracy and speed but none of these work provided a control solution to effectively sort out the CT with defect so that there will be no human intervention to sort and recycle the defective CT.



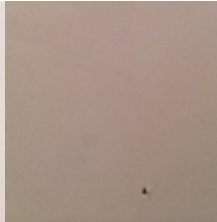

In this work, SVM classifier result provides an output information to a control system for effective sorting of the CTs with defects for

recycling the defective tiles. To achieve that, Proportional Integral Derivative (PID) controller and Direct Current (DC) motors are used in the sorting unit to open the gate at predefined distance when defect is detected in the CT. This will allow the CT with defect to be dropped on the conveyor belt to be return for reprocessing.

Most of the defects in CT production process that have statistical interest are the one that are found in the firing stage (Monday *et al.*, 2021). Some data collected from firing unit by firing unit worker in a CT factory is shown in Table 1.

The simulation in this work is based on the data collected West African Ceramic tiles company, Ajaokuta, Nigeria as is based on the four types of defect presented in in table 1.

**Table 1:** Major Defects in CT Firing Unit [Monday *et al.*, 2021]

Type	Diffused Glaze Crack (Crack I)	Capillary Crack (Crack II)	Pin-Hole	Hole
Occured in the kiln	Occurred in pre-heating due to excessive increasing rate of temperature, and then the glaze diffuses inside it in cooking area.	Occurred in cooling area due to excessive decreasing rate of temperature.	Occurred in cooking area due to excessive cooking.	Occurred in pre-heating and cooking area due to excessive absorption of CT's body moisture.
Defective images				

## MATERIALS AND METHODS

Figure 1 is the complete experimental set up of CT surface detection and classification system, it consist of the image acquisition sub-unit, the defect detection and classification sub-unit, and the sorting unit. The image acquisition unit uses position detection sensor and camera to capture

every CT coming in the Kiln, while and classification stage is done in the aid of MATLAB software in the computer and the sorting unit comprises of the PID controller and DC motor that sort defective tiles based on the output response of the classifier.

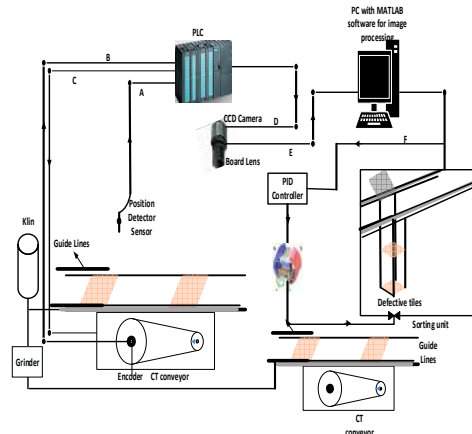


**Figure 1.** CTs' surface defects detection and classification experimental setup.

Figure 1 is the complete setup that explains the overall process of the system. CT been baked and dried coming out of the kiln fixed on the conveyor belt by guide lines. The position detector sensor will detect the edge of the tile then send a signal (A) to the programmable logic controller. The programmable Logic Controller (PLC) with the aid of the encoder on the rotor shaft of the motor begins to record the encoder numeration and mathematically. It relate the ratio to the distance of the tile on the conveyor when it received signal (B). The Conveyor motor will be stopped at predefined position under the camera when it received signal (C) and at that point the camera will receive signal (D) from the PLC to snap the surface of the CT. The analog signal of the captured image will be sent to the PC for processing and this is referred to as signal (E). The detection and classification scheme are achieved in the PC. The sorting unit responds to the output of the classifier via the PID controllers and the DC motors. Each of the defect properly classified opens its corresponding gate controlled by the DC motor to be dropped on the conveyor belt to be returned for reprocessing. A total of 230 CTs' images were acquired with 200 of them having different types of defects and 30 images with no surface defects being used as templates

### Defect Classification

The defect is detected and the Fourier features are extracted to train the Support Vector Machine (SVM) The choice of SVM is because of its ability to handle non-linear data point. Since the number of input features is more the One-Against-All SVM is used. (Hanzaei et al., 2017).

The kernel function is what SVM uses to show mapping. Hyper-plane shows the boundary between data samples of two classes.

$N$  given as:  $\{X_1, Y_1\}, \dots, \{X_N, Y_N\}$  is the

training sample and  $x_i \in R^m$  is the  $m$  dimensional feature vector representing the  $i^{th}$  training sample, and  $y_i \in \{-1, 1\}$  is the class label of  $x_i$ . A

hyper-plane which separates the classes in the feature space can be described by  $w^T x + b = 0$

. Where  $w \in R^m$  a vector is normal to the hyper-plane and  $b$  is a scalar. When the training samples are linearly separable, SVM yields the optimal hyper-plane that separates two classes with no training error, and maximizes the minimum distance from the training samples to the hyper-plane. The separating hyper-plane (described by  $w$ ) is determined by seeking the optimal margin between two classes. The width of the margin is

$\frac{2}{w \cdot w}$  The parameter pair  $(w, b)$  corresponding to the optimal hyper-plane is the solution to the following optimization problem (Kamani *at al.*, 2011)

The non-linear two-class SVM classifier as used in this method is express in figure 2. With the red points indicating data samples of one class and the blue points showing the data samples of the remaining classes. The red line is the support vector machine for the class of red point samples and the blue line is the support vector machine for the blue point samples. The black line is the optimized classification hyper-plan for these classes.

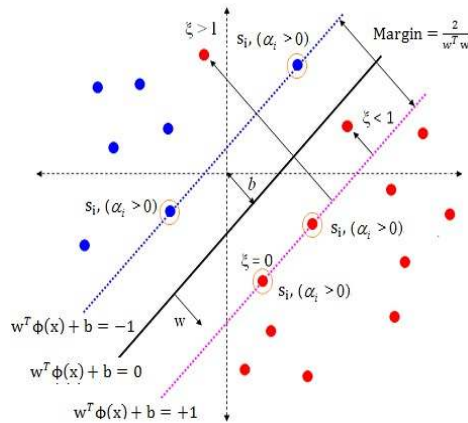


Figure 2: Non-Linear SVM classifier (Hanzaei et al., 2017).

The testing phase make used of one-against-all SVM classifier for multi-class classification. In this approach for each class an SVM is constructed by discriminating that class against the remaining classes ( $M-1$ ). The number of SVMs used in this approach is equal to number of classes ( $M$ ). A test pattern  $x$  is classified by using the winner-takes-all decision strategy. All the  $N$

$$y_i = \begin{cases} +1 & \text{if } c_i = k \\ -1 & \text{if } c_i \neq k \end{cases} \quad (1)$$

The examples with the desired output  $y_i = +1$  are called positive examples and the examples with the desired output  $y = -1$  are called negative examples. An optimal hyper-plane is constructed to separate  $N/M$  positive examples from  $N(M-1)/M$  negative examples (Kamani et al., 2011).

training examples are used in constructing an SVM for a class. The SVM for class  $k$  is constructed using the set of training examples and their desired outputs  $(x_i, y_i)$ . The desired output  $y_i$  for a training example  $x_i$  is defined as follows

#### The Automated Control Unit Model Solution

The model is controlled by the plant and this can be shown through the simplified control system in Figure 3.

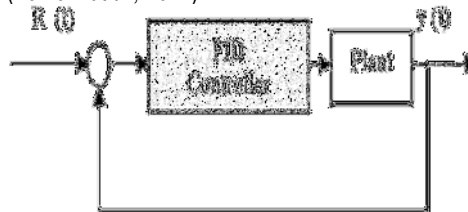


Figure 3: Simplified Control solution model

The plant is the motor whose output signal  $y(t)$ , the desired position  $R(t)$  will yields certain errors which will be injected into the Proportional-Integral-derivative (PID), the PID accept this error signal and generate a manipulated variable that acts on the system to get the desired output. The motor has different position response to step voltage input that exhibit behaves such as rise time, steady state,

peak overshoot and settling time. The behaviors of the motor are controlled by selecting the three gains of the PID controller, these gains modify the controller dynamically. The relationship between the controller input  $e(t)$  and the controller output  $u(t)$  that is applied to the motor armature is shown by the following relationship:

$$u(t) = kp \times e(t) + ki \times \int_0^t e(\tau) \times d\tau + kd \times \frac{de(t)}{dt} \quad (2)$$

Taking the Laplace transform of equation (2) will give the transfer function G(s):

$$G(s) = \frac{u(s)}{e(s)} = \left( kp + \frac{ki}{s} + kd \times s \right) \quad (3)$$

The transfer function in equation (3) is what shows the proportional, integral and derivative gains that the PID is made up of that carries out the compensation.

The DC motor converts electrical energy into mechanical energy and are used in industry control applications. DC motor gives good speed and position control respond and that makes it to be used in speed and position

control systems which needs high control requirements like high precision digital tools, rolling mill, double-hulled tanker etc. (Gani *at al.*, 2019).

The electric circuit and free body diagram of the DC motor is shown in Figure 4 while Table 2 is the assumed values of the physical parameters of the DC motor.

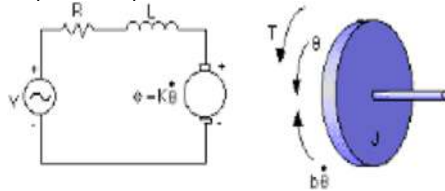


Figure 4: Electric circuit and free body diagram of DC motor.

Table 2: Assumed values for the physical parameters

Physical parameter	Assumed Values
Moment of inertia of the rotor (J)	0.01 kg.m <sup>2</sup> /s <sup>2</sup> .
Damping ratio of the mechanical system (b)	0.1 nms.
Electromotive force constant (k= ke = kt)	0.01 nm/amp
Electric resistance (R)	1 ohm.
Electric inductance (L)	0.5 H
Input (v)	Source Voltage.
Output (theta):	Position of shaft.
The rotor and shaft	Rigid

The motor torque T, is related to the armature current i, by a constant factor kt and the back e.m.f. is related to the rotational velocity as shown in equation (4)

$$T = kt \times i \text{ and } e = e.m.f = ke \times \dot{\theta} \quad (4)$$

From figure 4, combining Newton's law with Kirchoff's law the following equations can be obtain.

$$J \times \ddot{\theta} + b \times \dot{\theta} = k \times i, L \times \frac{di}{dt} + R \times i = V - k \times \dot{\theta}. \quad (5)$$

To obtain the transfer function, Laplace transforms can be used, expressing the modeling equations in terms of s.

$$S(J \times s + b) \times \theta(s) = k \times i(s) \quad (6)$$

$$(L \times s + R) \times i(s) = V - k \times s \times \theta(s).$$

By eliminating i (s) we can get the following open-loop transfer function, where the position is the output and the voltage is the input.

$$\frac{\theta}{V} = \frac{k}{(J \times s + b) \times (L \times s + R) + k^2} \quad (7)$$

Equation 7 shows the relationship between the input step voltage and the position at which the DC motor will open the gate. The gates are designed for 1 radian/seconds with design criteria of settling time less than 1 second and overshoot of not more than 2 %. This design is repeated for each of the gates.

## RESULTS AND DISCUSSION

Table 3 shows the transient response of the DC motor when a unit step signal is applied. Table 4 is the DC motor transient response characteristic when PID controller is used.

**Table 3:** The DC motor transient response characteristic

Characteristic	Data
Rise Time in seconds	1.0262
Settling Time in seconds	1.8623
Overshoot in percentage	0.0000
Peak in rad/second	0.0910
Peak Time in seconds	10.000
Steady state error	0.9900

From Table 3, shows the results obtained when DC motor was used alone, with a settling time of 1.8623 seconds, 0% overshoot

and 99% steady state error. Although it has a perfect overshoot but the steady state error was not good for the design specification.

**Table 4:** The DC motor with PID transient response characteristic

Characteristic	Data
Rise Time in seconds	0.1550
Settling Time in seconds	0.2343
Overshoot in percentage	0.5782
Peak in rad/second	1.0057
Peak Time in seconds	0.2887
Steady state error	0.0000

The settling time is 0.2343 seconds and the overshoot is 0.5782 percent, a steady state error of 0% was obtained. With PID controller the design specification of 1

rad/seconds was obtained, the overshoot has no effect on the system.

Figure 5 gives the graphical transient response when DC motor is used alone and when PID controller is used with DC motor.

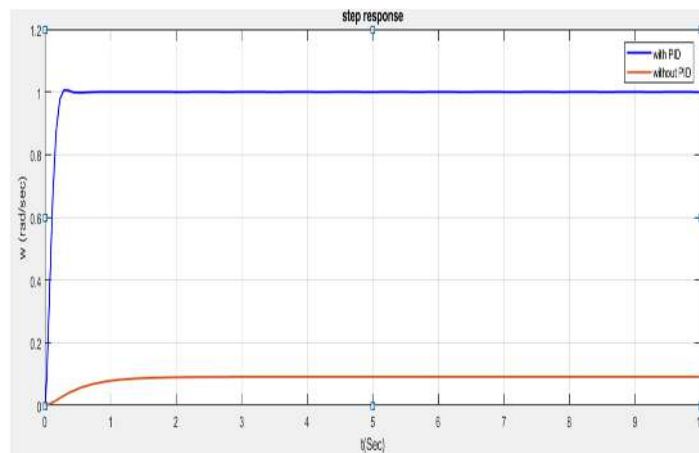


**Figure 5:** DC motor graphical transient response characteristic with and without PID controller

From the results obtained, we can deduced that the settling time of the DC motor is faster when PID controller is used with the DC motor. When PID controller is used with a DC motor angle of 1 rad/second will be obtained compared with when DC motor is used alone with 0.0910 rad/seconds.

Figures 6 through figure 9 show each defect with corresponding response of the gate. Figure 6 is crack I and gate 1 opening at specified design. Figure 7 shows Crack II, Figure 8 shows pin-hole and Figure 9 shows hole respectively.

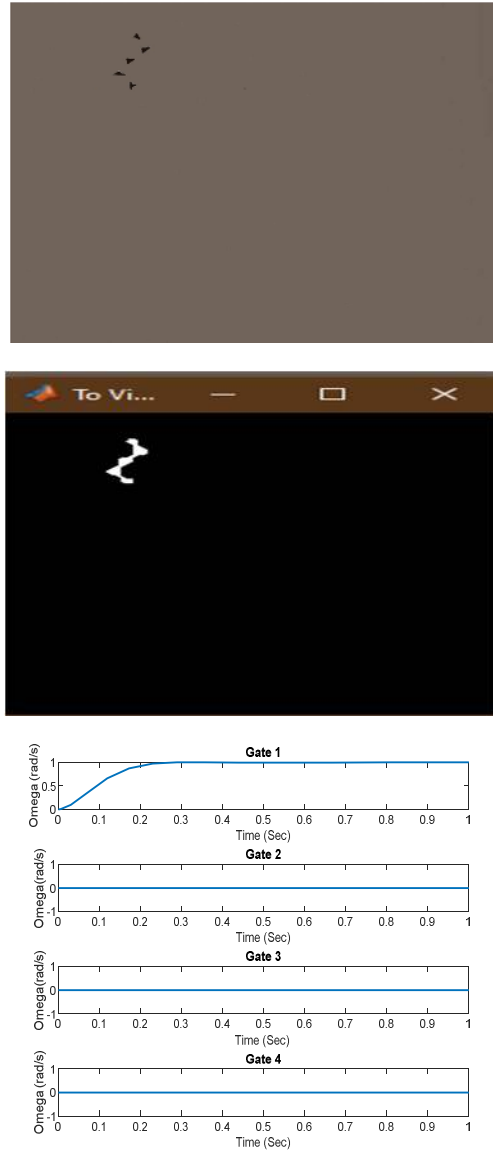


**Figure 6:** Gate 1 response to Crack I defect

In Figure 6, only gate 1 opens when defect type 1 was detected while the remaining three gate remain closed. The defective CT type 1 will pass through gate 1 with rising time at

0.1550s, settling time at 0.2343s and 0.5782 percent with the maximum distance of 1 radians per seconds.

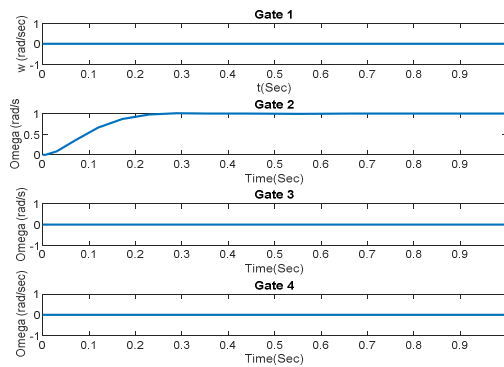
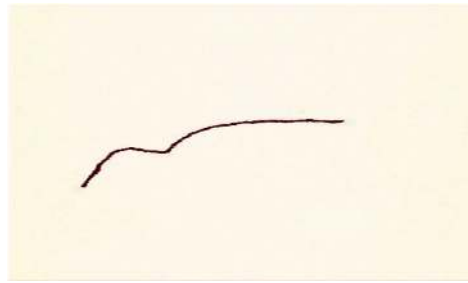


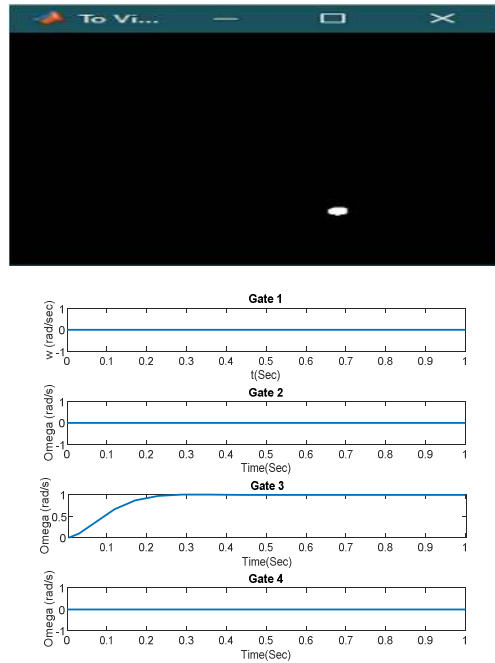
**Figure 7:** Gate 2 response to Crack II defect

In Figure 7 only gate 2 opens when defect type 2 was detected while the remaining three gate remain closed. The defective CT type 2 will pass through gate 2 with rising time at

0.1550s, settling time at 0.2343s and 0.5782 percent with the maximum distance of 1 radians per seconds.



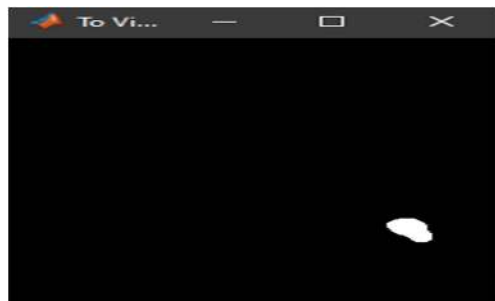




**Figure 8:** Gate 3 response to Pin-hole defect

In Figure 8 only gate 3 opens when defect type 3 called pin-hole was detected while the remaining three gate remain closed. The defective CT pin-hole will pass through gate 3

with rising time at 0.1550s, settling time at 0.2343s and 0.5782 percent with the maximum distance of 1 radians per seconds.



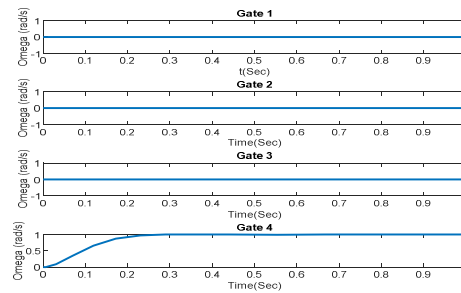


Figure 9: Gate 4 response to Hole defect

In Figure 9 only gate 4 opens when defect type 4 called hole was detected while the remaining three gate remain closed. The defective CT called hole will pass through gate 4 with rising time at 0.1550s, settling time at 0.2343s and 0.5782 percent with the maximum distance of 1 radians per seconds.

The result shows that each of Gate 1, 2, 3 and 4 exhibit the same characteristic response with DC motor and PID controller with the settling time of 0.2343s and overshoot of 0.5782%. When gate 1 opens in response to Crack I, the remaining gates remain closed. Only one gate responds to the corresponding defect type at a time and with the control solution the gates are been controlled and opened at the required position.

## CONCLUSION

An automated control solution was also introduced to return CT with defects to for reprocessing depending on the degree of tolerance of the defects. And for this to be achieved the sorting unit has a gate that is controlled to open automatically at 1 radian/seconds when defect is detected. The gate is controlled by a DC motor and PID controller that has a settling time of 0.2343s and overshoot of 0.5782 %.

## REFERENCES

- Hanzaei, S. H., Afshar, A., & Barzandeh, F. (2017). Automatic detection and classification of the ceramic tiles' surface defects. *Pattern Recognition*, 66, 174-189.
- Meena, Y., & Mittal, A. (2013). Blobs and Cracks Detection on Plain Ceramic Tile Surface. *International Journal of Advanced Research in Computer*

*Science and Software Engineering*, 3(7)

- Junmo Kim, J. W. Fisher, A. Yezzi, M. Cetin and A. S. Willsky, "A nonparametric statistical method for image segmentation using information theory and curve evolution," in IEEE Transactions on Image Processing, vol. 14, no. 10, pp. 1486-1502, Oct. 2005, doi: 10.1109/TIP.2005.854442.
- Latif-Amet, A., Ertüzün, A., & Erçil, A. (2000). An efficient method for texture defect detection: sub-band domain co-occurrence matrices. *Image and Vision computing*, 18(6-7), 543-553.
- Iivarinen, J. (2000). Surface defect detection with histogram-based texture features. Paper presented at the Intelligent robots and computer vision xix: Algorithms, techniques, and active vision.
- Mallik-Goswami, B., & Datta, A. K. (2000). Detecting Defects in Fabric with Laser-Based Morphological Image Processing. *Textile Research Journal*, 70(9), 758-762. <https://doi.org/10.1177/004051750007000902>
- S. Vasilic and Z. Hocenski, "The Edge Detecting Methods in Ceramic Tiles Defects Detection," 2006 IEEE International Symposium on Industrial Electronics, 2006, pp. 469-472, doi: 10.1109/ISIE.2006.295640
- Monday F.O., Salawudeen A.T., Zubair Z. O., & Nkiru E. (2021). Development of Automated Ceramic Tiles Surface Defect Detection and Classification System. *International Journal of Innovations in Engineering Research and Technology*, 8(08), 200-209



Kamani, P., Afshar, A., Towhidkhan, F., & Roghani, E. (2011). Car body paint defect inspection using rotation invariant measure of the local variance and one-against-all support vector machine. Paper presented at the 2011 First International Conference on Informatics and Computational Intelligence.

Gani, M. M., Isalm, M. S., & Ullah, M. A. (2019). Modeling and Designing a Genetically Optimized PID Controller for Separately Excited DC Motor. Paper presented at the 2019 International Conference on Electrical, Computer and Communication Engineering (ECCE).